

MECHANISM ANALYSIS OF BIT STICK-SLIP VIBRATION IN NEAR-HORIZONTAL DRILLING

Xu, B. L.^{*,**}; Zhang, X. D.^{***,#}; Ye, S. X.^{****} & Gan, Y. P.^{*,**}

^{*} Key Laboratory of Xinjiang Coal Resources Green Mining, Ministry of Education (Xinjiang Institute of Engineering), Urumqi 830023, China

^{**} School of Safety Science and Engineering, Xinjiang Institute of Engineering, Urumqi 830023, China

^{***} College of Mechanical and Electronic Engineering, Shandong University of Science and Technology, Qingdao 266590, China

^{****} Xi'an Research Institute, China Coal Technology & Engineering Group, Xi'an 710077, China

E-Mail: zhangxiaodi@sdust.edu.cn (# Corresponding author)

Abstract

This study develops a numerical model using ABAQUS to investigate the stick-slip vibration mechanism of a near-horizontal drilling bit in underground mines, incorporating bit-rock cutting, drill string-hole wall interaction, and gravity. Key factors include feed speed, rotational speed, drill string length, and rock properties. Results show that stick-slip vibration consists of slow loading, sticking, slip, and high-speed rotation sections and is coupled with axial vibration. Higher feed speed increases torsional energy storage time, thereby prolonging the sticking section. Higher rotational speed raises the peak velocity of the bit during stick-slip, which can exceed twice the driving speed. Drill string flexibility is a root cause; shorter strings with higher stiffness reduce sticking tendency. Average drilling speed decreases with increasing string length, though the reduction rate diminishes. Increased rock hardness prolongs the sticking phase, but the increment gradually levels off. These findings provide a theoretical reference for safe and efficient near-horizontal drilling in underground mines.

(Received in February 2026, accepted in April 2026. This paper was with the authors 2 weeks for 2 revisions.)

Key Words: Near-Horizontal Drilling, Bit, Stick-Slip Vibration, Mechanism, Axial Vibration

1. INTRODUCTION

Advanced drilling is a necessary channel for exploring and controlling geological disasters before underground mining [1]. In conventional drilling, drill pipes are used to drive the polycrystalline diamond cutter (PDC) bit for rock-breaking drilling. A deep drilling distance can easily lead to insufficient torsional stiffness of the drill pipes, excessive cutting depth of the PDC bit under high drilling pressure, or high cutting torque requirements when the drill bit encounters hard or complex formations. As a result, the drill bit speed may drop below the orifice speed or even become stuck. At this point, the orifice continues to apply torque, and the drill pipe accumulates rock-breaking energy due to torsion. When this reserve energy reaches the rock-breaking threshold of the drill bit, it is suddenly released, driving the drill bit at the bottom of the hole to rotate at a speed far exceeding the preset orifice speed [2]. The torsional and stick-slip vibrations of the drill bit lead to serious impact collision between the drill bit and the rock, which can cause abnormal failure of the PDC cutter and signal failure of the MWD instrument, thereby increasing drilling cost and reducing efficiency [3].

To better meet the needs of deep drilling and complex formation for efficient and safe construction, researchers are focusing on comprehensive control technology based on the active control of orifice parameters and passive vibration suppression of bottomhole vibration reduction equipment [4], a technology widely used in related fields. Regardless of the type of control technology, the theoretical basis for its development is the accurate identification of the occurrence mechanism and response characteristics of stick-slip vibration of the bottom bit. However, stick-slip vibration involves many coupling factors, such as weight on bit (WOB), torque, friction characteristics, and formation characteristics, bringing great

challenges to the dynamic modelling, state identification, and active and passive control of drill string systems.

On this basis, researchers have carried out extensive research on the dynamic characteristics of stick-slip vibration under multi-field coupling [5-7]. However, due to the multi-field complex coupling effect in actual near-horizontal hole drilling, current theoretical results still have problems, such as few coupling variables and large differences between theoretical and actual values. Therefore, revealing the occurrence mechanism of bit stick-slip vibration during near-horizontal hole drilling has great theoretical significance for guiding safe and efficient construction.

This study establishes a numerical model of a horizontal drilling system, which simultaneously considers interactions between bit and formation cutting and between drill string and hole wall, the stiffness of the drill string, and the multi-field coupling of formation characteristics. The purpose of this study is to identify the mechanism of stick-slip vibration of a near-horizontal drilling bit and then provide reference for the application development and construction optimization of near-horizontal hole advanced drilling technology.

2. STATE OF THE ART

The stick-slip vibration of drill bit depends on bit-rock interaction and drill string elasticity. Nonlinear dynamics has been widely applied to study this phenomenon. Lobo et al. [8] developed a nonlinear drill-rock coupling model with random rock strength, capturing drill string torsional vibration. Moharrami et al. [9] built a full finite element (FE) model of the drill string, bit, and rock, incorporating geometric nonlinearity, element number, and torsional-longitudinal coupling. Modal analysis yielded natural frequencies and modes, which were validated against stick-slip experiments. De Moraes and Savi [10] proposed a four-degree-of-freedom non-smooth model for torsional-longitudinal-transverse coupling, studying bit bounce, stick-slip, and torsion under varying drilling parameters, with their results matching field tests. Richard et al. [11, 12] introduced a two-degree-of-freedom model with a delay term for rock cutting and crushing, identifying that bit circumferential rotation and torsion induce stick-slip, and argued that increased friction torque is a system response, not a direct bit-rock effect. Sharma et al. [13] presented two nonlinear coupled torsional rock interaction models based on velocity-weakening friction and state-dependent delayed friction to analyse stick-slip severity in hard rock. These models evaluate drilling pressure, rotational speed, friction parameters, and uniaxial compressive strength. Although nonlinear dynamics reveals macroscopic influences on stick-slip, it cannot capture microscopic bit-rock cutting interactions, and idealized mathematical models poorly represent highly complex drilling systems.

With the advances in computer simulation, FE and discrete element methods (DEMs) are increasingly used to study torsional and stick-slip vibrations, thereby clarifying microscopic mechanisms. DEM with particle flow simulates particle migration and failure [14], and after bonding, it models rock crushing by the bit. Zhang et al. [15, 16] developed a single PDC cutter rock-breaking model using particle flow, identifying the effects of rotational speed and WOB on stick-slip, and proposed torsional and axial impact mitigation strategies. Huang et al. [17] coupled a lumped-mass drill string model with a discrete element bottomhole assembly to study bit dynamics, which was validated by experiments. Jamie et al. [18] used LS-DYNA to simulate PDC cutter rock cutting and chip formation, determining the critical cutting depth for brittle-ductile transition, clarifying the role of cutting depth in stick-slip, and confirming explicit FE feasibility. Xiang et al. [19] incorporated a state-dependent delayed cutting-friction model into FE analysis to characterize drill-rock interaction and studied WOB and rotational speed effects on drill string nonlinear vibration. However, these studies

insufficiently considered drill string system effects on bit cutting. Liu et al. [20] established an axial-lateral-torsional coupled nonlinear FE model for ultra-high-temperature high-pressure curved wells, accounting for wellbore trajectory, constraints, bit-rock interaction, and temperature/ pressure-dependent drilling fluid properties. Moreover, they explored the effects of rotational speed, string length, and WOB on stick-slip. Analysing 3-D acceleration signals from drilling experiments, Zhang et al. [21] found that bit stick-slip aggravates drill string torsional vibration, as verified by a fully coupled FE model. Wang et al. [22] developed an FE model that includes bit-wellbore impact friction, fluid-solid coupling, bit-rock interaction, and gravity, revealing that torsional excitation worsens bit angular velocity fluctuations, while axial excitation has negligible effect. Nevertheless, none of the abovementioned studies systematically considered the synergistic coupling between bit cutting and flexible drill string interaction.

Theoretical and numerical studies have likewise analysed axial and torsional excitations on bit stick-slip. Based on vibration theory, Li et al. [23, 24] established a torsional impact drilling model accounting for drill pipe energy dissipation. Through theory and field tests, they confirmed the advantages of torsional impact drilling at high WOB and low rotational speed and found that string damping and stiffness significantly affect torsional and axial responses, respectively. Zhang et al. [25] used DEM to simulate PDC tooth drilling in gravelly sandstone and found that composite impact loads effectively suppress tooth surface vibration. Xi et al. [26] numerically studied axial, torsional, and torsional-longitudinal coupled percussive drilling and showed that increasing impact frequency reduces bit vibration; under coupled impact, the best penetration rate occurs at a 25 % phase difference. However, these studies apply excitation loads directly to the rock-breaking tool without considering drill string-tool interaction.

In summary, current research has two main shortcomings: (1) Nonlinear dynamics theory cannot accurately characterize the highly complex drilling mechanical behaviour nor reveal the microscopic stick-slip mechanism. (2) Numerical simulation methods, while capable of revealing mechanisms, often neglect bit-rock cutting interaction, drill string-borehole wall contact, string flexibility, and gravity. Consequently, understanding of the microscopic mechanism of bit stick-slip vibration in near-horizontal drilling remains incomplete.

The rest of this paper is organized as follows. Section 3 details the analysis model, material parameters, and simulation parameter settings based on ABAQUS, including different feed speed, rotational speed, drill string length, and rock parameters. Section 4 analyses the relationship between different factors and stick-slip vibration. Section 5 concludes the paper.

3. METHODOLOGY

3.1 Geometric model

First, the following basic assumptions are made for the analysis model:

- (1) The horizontal drill string is in a linear elastic state, the connection of the coupling is not considered, and small deformations are assumed.
- (2) The cross sections of the horizontal drill string and the borehole are circular.
- (3) The borehole is not deformed and processed into a rigid body.
- (4) The initial position of the horizontal drill string coincides with the borehole axis and maintains a linear equilibrium state, taking the isotropic assumption.
- (5) The horizontal drill string is bent and deformed under the actions of gravity, centrifugal force, and feed force, which may bring it into contact with any position on the inner wall of the borehole, taking into account the influence of dynamic and static friction.
- (6) The inertia and damping forces in the transient effect are neglected.

3.2 Rock properties

The rock model adopts the linear Drucker-Prager model. General coal measures strata, especially near coal seams, are mainly mudstone, sandy mudstone, and sandstone. The rock parameters listed in Table III are based on the relevant results of rock mechanics tests for general coal measures strata [27].

Table III: Main parameters of the rock.

Lithologic characters	Density (kg/cm ³)	Compressive strength (MPa)	Elastic modulus (GPa)	Poisson ratio	Force of cohesion (MPa)	Angle of internal friction (°)
Coal	1.38	10.08	2.83	0.20	4.57	35.21
Mudstone	2.20	37.70	14.69	0.25	11.74	27.00
Sandy mudstone	2.51	47.10	17.50	0.25	13.28	29.00
Fine sandstone	2.873	91.03	21.22	0.16	17.15	34.03
Coal	1.38	10.08	2.83	0.20	4.57	35.21

3.3 Simulation scheme

As shown in Fig. 1, n is the rotational speed of the power head, v_h is the feed speed of dynamic head, and L and the length of the drill string. The values of n , v_h , and L are shown in Table IV.

Table IV: Simulation variables.

n (rpm)	v_h (mm/s)	L (m)
50, 75, 100, 150	5, 10, 15, 20	10, 20, 40, 100

4. RESULTS AND DISCUSSION

4.1 Occurrence of stick-slip vibration

As shown in Fig. 2, the occurrence of typical stick-slip vibration is analysed using the example of a 150 rpm rotational speed and 20 mm/s feed speed when drilling fine sandstone:

(1) Slow loading section: At 0–0.5 s, power head speed gradually increased from 0 to 150 rpm. The actual drilling conditions, actual drilling of the first rotary power head, and the pressurized feed are all the same at this time.

(2) Initial rebound section: Displacement is applied at 0.5 s. As shown in Fig. 3, owing to rock hardness, the drill bit cannot penetrate and instead rebounds in reverse, inducing axial vibration. At 0.65 s, maximum rebound speed reaches 80 mm/s, then gradually decreases due to drill string damping. At 0.75 s, rebound speed becomes zero at a maximum rebound displacement of 14.7 mm. Subsequently, the elastic restoring force drives the bit forward until it reaches the bottomhole, and cutting commences at 0.85 s.

(3) Stuck section: Before 1.58 s, the parameters of each drilling phase are unstable, and the axial rebound amplitude is large. After 1.58 s, it enters a relatively stable stuck section. At this time, the bit speed and axial speed of the bit gradually decrease, and the bit begins to enter the stuck stage.

(4) Stick section: The bit enters the stick section at about 1.65 s. At this stage, the angular velocity and axial velocity of the bit are both 0, which means the bit cannot be drilled at this stage. The torque of the drill bit gradually increases, and the drill string system begins to store energy. The torque increases from the minimum value of 0 entering the stick section to about 2500 N·m at the end of the stick section. During this period, the axial force of the drill bit by the formation is also at a high level, fluctuating between 15 and 45 kN.

(5) Slip section: The accumulated torque reaches the maximum value of 2500 N·m at about 1.95 s, and the drill bit reaches the rock threshold rupture value. After the rock is broken, the angular velocity of the drill bit increases rapidly from 0 to 30 rad/s, which is about twice the set speed (15.7 rad/s) of the orifice pusher.

(6) High-speed rotation section: The axial force of this section of the drill bit is small, between 0 and 10 kN. The drill bit cannot be effectively pressed into the formation, and the friction torque from the formation is small, so the drill bit maintains a certain angular velocity in a short time.

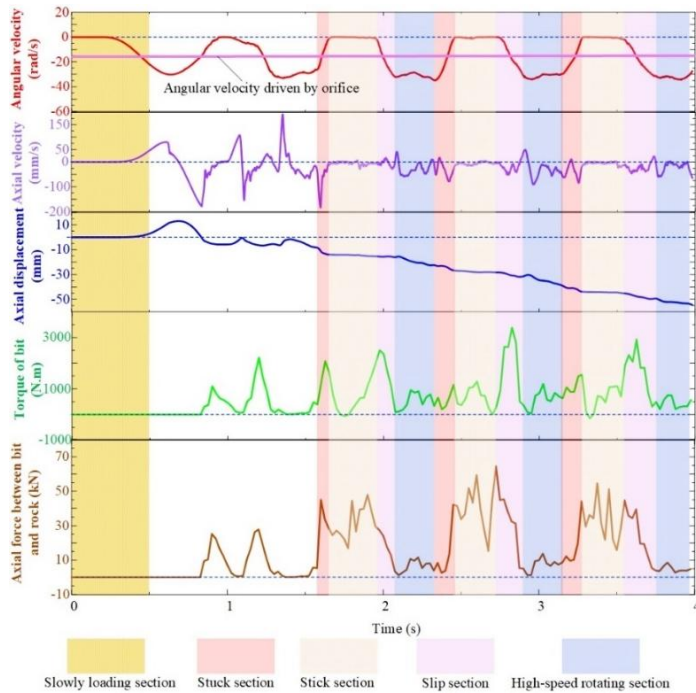


Figure 2: Time history diagram of various motion parameters of the drill bit.

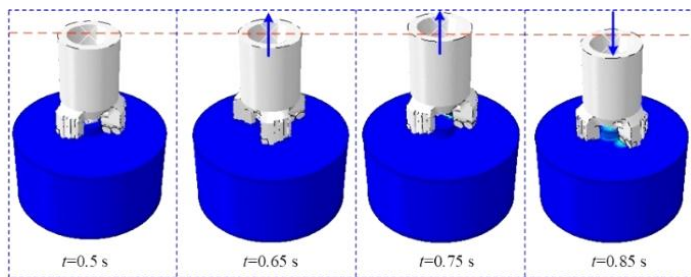


Figure 3: Location map of the drill bit at different times.

4.2 Interaction between stick-slip vibration and axial vibration

According to the analysis of results in Section 4.1, the stick-slip vibration is accompanied by the axial vibration. The rotational speed of 150 rpm and feed speeds of 5, 10, 15, and 20 mm/s are set to further analyse their interaction. Since the results at the 15 mm/s feed rate are similar to those of the 20 mm/s rate used in the previous analysis of the stick-slip vibration, the simulation results at low feed rates are analysed. As shown in Figs. 4 a and 4 b, the drill string is in the initial oscillation region in the first 1.5 s, and the state is unstable; after 1.5 s, the rotational speed of the drill string is at the maximum value in the forward direction, and the rotational speed begins to decrease due to the damping motion. As the rotational speed continues to approach the hole drive angle, the axial vibration gradually approaches 0, and then begins to reversely accelerate the drill bit to come gradually into contact with and press

into the bottom of the hole. This, in turn, brings greater damping to the rotation of the drill bit, and the rotational speed begins to decrease gradually.

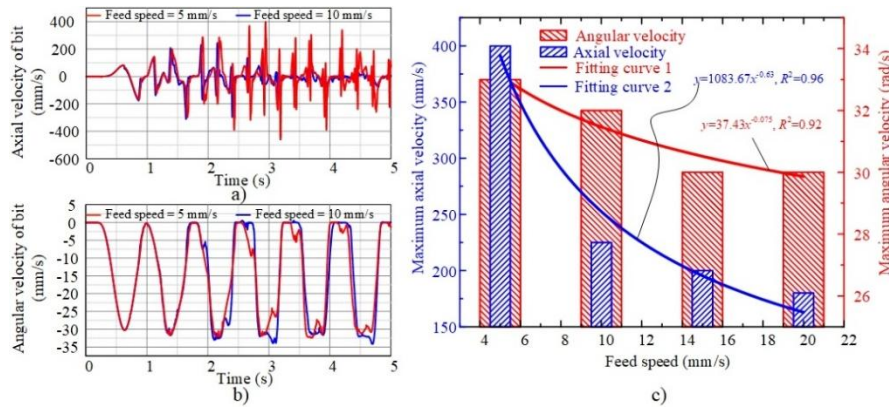


Figure 4: Relationship among axial vibration, torsional vibration, and feed speed of the drill bit.

A comparison of the two curves in Fig. 4 a reveals that the axial vibration amplitude is larger when the feed rate is lower. When the feed speed is 5 mm/s, the axial vibration amplitude is 400 mm/s; when the feed speed is 20 mm/s, the axial vibration amplitude decreases to 180 mm/s, and the decline curve shows a negative exponential type. As shown in Fig. 4 c, the fitting relationship between maximum axial velocity and feed speed is as follows:

$$y = 1083.67x^{-0.63} \quad (1)$$

For the peak angular velocity, when the feed rate is 5 mm/s, the axial vibration amplitude is 33 rad/s, which decreases with the increase of feed rate. When the feed speed is 20 mm/s, the axial vibration amplitude decreases to 30 rad/s, with a decrease of only 9.09%. This indicates that the increase of the feed speed has little effect on the angular velocity. As shown in Fig. 4 c, the fitting relationship between maximum angular velocity and feed speed is as follows:

$$y = 37.43x^{-0.075} \quad (2)$$

4.3 Effect of feed speed

Based on the analysis of the influence of a 4.2 mm/s feed speed on angular velocity, further analysis in Fig. 5 shows that at the same speed, a higher feed speed leads to a longer viscosity time in the single stick section of the drill. When the feed speed is 5 mm/s, the time length of single stick section is 0.1 s; at 20 mm/s, the time length of the stick section increases to 0.3 s. Therefore, the time length of a single stick section is positively correlated with the feed speed, and the fitting relationship between time length of stick section and feed speed is as follows:

$$y = 0.05 + 0.013x \quad (3)$$

As shown in Fig. 5, for the axial compression of the drill string, the greater the feed speed, the greater the compression of the drill string at the same time, and the corresponding compression is also larger. The analysis will be used further in the buckling state of the drill string in the next section. When the feed speed is 5 mm/s and the simulation time is 4 s, the axial compression of the drill string is 5 mm. When the feed rate is 20 mm/s and the simulation time is 4 s, the axial compression of the drill string is 20 mm. Thus, the axial compression of the drill string is positively correlated with the feed rate. The fitting relationship between compression of drill string and feed speed is:

$$y = 2.55 + 0.63x \quad (4)$$

In summary, the greater the feed speed, the greater the volume of rock to be cut per unit time. This finding means that the greater the torque and energy of the broken rock, the longer the time required for the torsional energy storage of the drill pipe at the same speed.

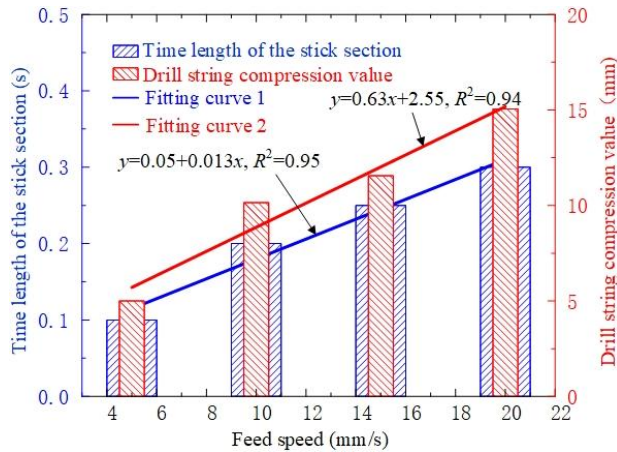


Figure 5: Relationship between stick-slip vibration and feed speed.

4.4 Effect of rotational speed

The working conditions of fine sandstone with a uniaxial compressive strength of 91.03 MPa and drill string length of 100 m were selected for research. The rotational speed of the orifice was set to 50, 75, 100, and 150 rpm. The time history of the rotational speed of the drill bit at the bottom of the hole is shown in Fig. 6 a. The figure shows that the peak speed of the drill bit increases significantly with the increase of orifice drive speed, but there is no significant change in the time length of the stick section. The ratio of the peak speed of the drill bit at the bottom of the hole to the driving speed of the hole is extracted, as shown in Fig. 6 b. When the driving speed of the hole is 50, 75, 100, and 150 rpm, the ratio of bit maximum rotational (*BMR*) speed and rotational speed of power head (*RHD*) is 1.93, 1.92, 1.93, and 2.1 respectively, and the ratio is basically unchanged. Therefore, by reducing the speed, the stick-slip vibration intensity of the drill bit at the bottom of the hole and the impact of the drill bit can be reduced.

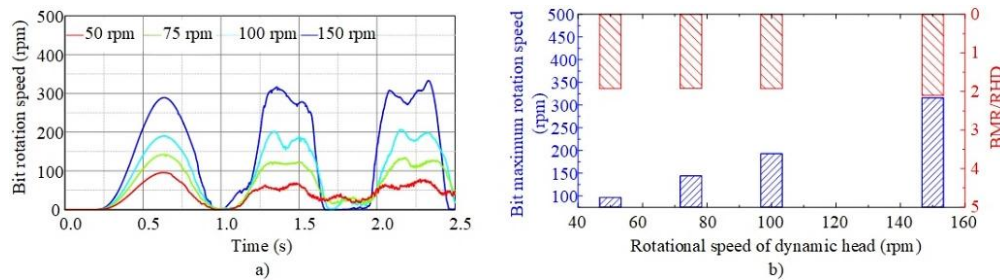


Figure 6: Relationship between stick-slip vibration and rotational speed.

4.5 Effect of drill string length

Fine sandstone with a uniaxial compressive strength of 91.03 MPa was selected as the research object. The equivalent length was obtained by changing the stiffness and mass of the drill string in the simulation model. The motion state of the drill bit was studied when the lengths of the drill string were 10, 20, 40, and 100 m. As shown in Fig. 7 a, when the length of the drill string is 10 m, the displacement of the drill bit basically coincides with the displacement of the orifice feed, indicating that the stick-slip vibration of the drill string system does not affect the drilling efficiency. However, when the length of the drill string becomes longer, due to the increased flexibility of the drill string and the increased stick-slip vibration intensity, the displacement curve of the drill bit lags behind the orifice feed displacement curve. This result indicates that the length of the drill string affects the drilling speed, resulting in a decrease in the average drilling speed.

Furthermore, the relationship among average drilling speed, time of the stick section, and length of the drill string was analysed. As shown in Fig. 7 b, the average drilling speed decreases with the increase of the length of the drill string, but the decrease gets smaller and smaller. When the lengths of the drill string are 10, 20, 40, and 100 m, the corresponding average drilling speeds are 20, 18.5, 17.8, and 15.7 mm/s, respectively. When the length of the drill string is 100 m, the average drilling speed decreases by 21.5 % compared with when the length is 10 m. The fitting relationship between average drilling speed and length of drill string is as follows:

$$y = 5.89e^{\frac{-x}{47}} + 15 \quad (5)$$

As shown in Fig. 7 b, the time length of the stick section of the bit increases linearly with the increase of the length of the drill string. When the lengths of the drill string are 10, 20, 40, and 100 m, the time length of the stick section is 0, 0.05, 0.1, and 0.3 s. The flexibility of the drill string can also be cited as one of the root causes of stick-slip vibration. When the length of the drill string is short, the stiffness of the drill string is large, and the drill bit does not stick easily. The fitting relationship between time length of the stick section and length of drill string is as follows:

$$y = 0.0032x - 0.026 \quad (6)$$

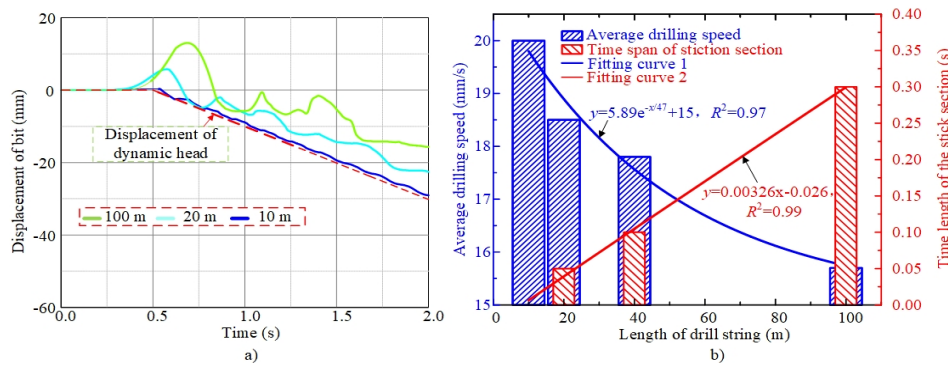


Figure 7: Relationship between stick-slip vibration and drill string length.

4.6 Effect of rock parameters

According to extensive practical engineering experience in near-horizontal advanced drilling in underground mines, the harder the stratum is, the more severe the pressure jitter of the drilling rig's rotary table during drilling will be, which will, in turn, cause the fierce lateral and axial vibration of the drill string system. To examine the influence of different formation characteristics on the stick-slip vibration of the drill bit during drilling, the feed rate of the orifice is set to a constant speed of 20 mm/s, and the rotational speed of the orifice is set to 150 rpm (the corresponding angular velocity is 15.7 rad/s). The parameters of coal, mudstone, sandy mudstone, and fine sandstone are input according to Table III.

Figs. 8 a and 8 b illustrate the time history diagram of the angular velocity and absolute displacement of the drill bit under different formation hardness. In particular, the change of rock hardness does not affect the angular velocity amplitude of the stick-slip vibration of the drill bit. The angular velocity peaks corresponding to the rock compressive strengths (σ_c) of 10.08, 3.77, and 9.1 MPa are 31.5, 31.6, and 31.55 rad/s, respectively, which are about twice the angular velocity value set by the orifice rotation. However, the time of the stick section in a single stick period corresponds to the uniaxial compressive strengths of 10.08, 37.7, 47.1, and 91 MPa, which are 0.05, 0.2, 0.22, and 0.27 s, respectively. When feed speed is 20 mm/s and rotational speed is 150 rpm, as shown in Fig. 8 c, the fitting relationship between the time length of the stick section and the compressive strength of the drilled rock is as follows:

$$y = 0.33 \ln(0.51 \ln x) \quad (7)$$

Fig. 8 c shows that the time length of the stick section increases with the increase of rock hardness. The drill string needs a longer time to accumulate energy when the orifice drive speed is constant because the harder the rock is, the greater the energy required to break it. However, the trend of the increase in the time length of the stick section tends to be gradual with the increase of hardness. The reason is that as hardness increases, the stick-slip vibration will cause axial vibration, which when coupled with the compression characteristics of the drill string itself results in the bottom of the hole. The drill bit cannot be pressed into the formation according to the feed rate of the orifice, and the decrease in its drilling speed leads to a linear increase in rock-breaking energy with hardness.

The influence of the increase of formation hardness on drilling efficiency is analysed as well, and the average drilling speed from the beginning of drilling ($t = 0.5$ s) to the end of simulation ($t = 2.5$ s) is analysed (shown in Fig. 8 b). As shown in Fig. 8 c, average drilling speed decreases greatly with the increase of formation hardness. The average drilling speed corresponding to the uniaxial compressive strengths of 10.08, 37.7, 47.1, and 91 MPa are 19.5, 15.85, 15, and 13.85 mm/s, respectively. The fitting relationship between average drilling speed and compressive strength of the drilled rock is as follows:

$$y = -8.5 \ln(0.04 \ln x) \tag{8}$$

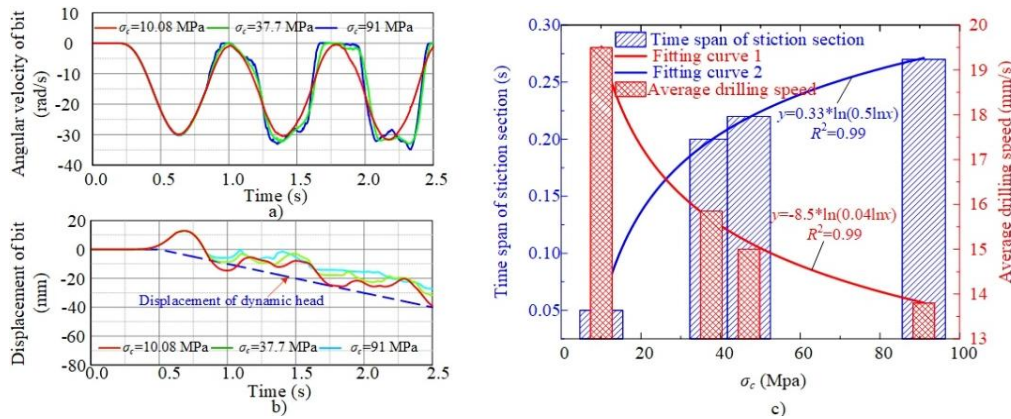


Figure 8: Relationship between stick-slip vibration and rock parameters.

5. CONCLUSION

In this study, a numerical model of a drilling system is established, considering drill bit-rock cutting interaction, drill string-hole wall interaction, drill string flexibility, and gravity effects. Additionally, the occurrence of stick-slip vibration and its interaction mechanism with axial vibration are investigated. Sixteen groups of numerical calculations are carried out by changing the rotational speed, feed speed, drill string length, and rock properties. Finally, the change curve of bit speed under different variables and their correlations are obtained. The conclusions are as follows:

(1) Stick-slip vibration is divided into four stages: stuck, stick, slip, and high-speed rotation. Axial vibration of the drill bit affects the indentation degree and anti-torque, serving as one of the main internal causes of stick-slip vibration.

(2) The greater the feed speed, the greater the rock-breaking torque and energy demand, and the longer the torsional energy storage time, thereby extending the stick section. With greater feed speed, the peak speed of the drill bit can exceed twice the speed of the orifice.

(3) Drill string flexibility is a major factor contributing to stick-slip vibration. The shorter the drill string, the greater the stiffness, and the lower tendency to stick. The average drilling speed decreases with the increase of drill string length, but the decrease is slow.

(4) When rock hardness increases, the stick section extends but the growth rate slows down. Higher hardness leads to the coupling of axial vibration and drill string compression,

which causes the actual drilling speed to decrease. However, the rock-breaking energy does not increase linearly with the hardness.

This study examines the relationship between stick-slip vibration intensity and rotational speed, feed speed, drill string length, and rock properties and proposes a strategy to suppress the stick-slip vibration intensity by changing drilling parameters. The results provide theoretical support for reducing the stick-slip vibration intensity of drill bit, reducing PDC cutter wear, and improving drilling efficiency. However, since the constant friction coefficient is adopted, the influence of horizontal hole drilling slag accumulation is not considered. Therefore, in future research, the drilling slag migration model could be coupled with this model so that research results are more consistent with engineering practice.

ACKNOWLEDGEMENT

This study was supported by the Automatic Research Fund of Key Laboratory of Xinjiang Coal Resources Green Mining (Grant No. KLXGY-Z2608), and the Doctoral Start-up Fund of Xinjiang Institute of Engineering (Grant No. 2025XGYBQJ55).

REFERENCES

- [1] Xu, B. L.; Zhang, X. D.; Ye, S. X.; Guo, S. S. (2025). Collapsed particles velocity analysis in drill hole based on CFD–DEM, *International Journal of Simulation Modelling*, Vol. 24, No. 4, 623-634, doi:[10.2507/IJSIMM24-4-741](https://doi.org/10.2507/IJSIMM24-4-741)
- [2] Richard, T.; Germain, C.; Detournay, E. (2004). Self-excited stick-slip oscillations of drill bits, *Comptes Rendus. Mecanique*, Vol. 332, No. 8, 619-626, doi:[10.1016/j.crme.2004.01.016](https://doi.org/10.1016/j.crme.2004.01.016)
- [3] Ertas, D.; Bailey, J. R.; Wang, L.; Pastusek, P. E. (2014). Drillstring mechanics model for surveillance, root cause analysis, and mitigation of torsional vibrations, *SPE Drilling & Completion*, Vol. 29, No. 4, 405-417, doi:[10.2118/163420-PA](https://doi.org/10.2118/163420-PA)
- [4] Lu, C.-D.; Huang, H.-Y.; Sun, H.; Jin, F.-X.; Sato, D.; Wu, J.-D. (2026). Suppressing torsional drill-string vibrations considering high- and low-frequency disturbances by model reference adaptive control with equivalent-input-disturbance method, *ISA Transactions*, Vol. 169, 683-693, doi:[10.1016/j.isatra.2025.12.028](https://doi.org/10.1016/j.isatra.2025.12.028)
- [5] Real, F. F.; Lobo, D. M.; Ritto, T. G.; Pinto, F. A. N. C. (2018). Experimental analysis of stick-slip in drilling dynamics in a laboratory test-rig, *Journal of Petroleum Science and Engineering*, Vol. 170, 755-762, doi:[10.1016/j.petrol.2018.07.008](https://doi.org/10.1016/j.petrol.2018.07.008)
- [6] Wang, L.; Han, Z.-B.; Wang, J.-D.; Guo, L.-R.; Li, R. (2024). Analysis on the dynamic characteristics of stick-slip vibration in deep well drill string system, *Thermal Science*, Vol. 28, No. 2, Part A, 1161-1167, doi:[10.2298/TSCI230721040W](https://doi.org/10.2298/TSCI230721040W)
- [7] Choe, Y.-M.; Kim, G.-S.; Kim, I.-S.; Cha, J.-C.; Ri, K.-W.; Han, Y.-S.; Kang, C.-H. (2023). Influence of torsional stick-slip vibration on whirl behavior in drill string system, *Geoenergy Science and Engineering*, Vol. 227, Paper 211931, 23 pages, doi:[10.1016/j.geoen.2023.211931](https://doi.org/10.1016/j.geoen.2023.211931)
- [8] Lobo, D. M.; Ritto, T. G.; Castello, D. A. (2020). A novel stochastic process to model the variation of rock strength in bit-rock interaction for the analysis of drill-string vibration, *Mechanical Systems and Signal Processing*, Vol. 141, Paper 106451, 17 pages, doi:[10.1016/j.ymssp.2019.106451](https://doi.org/10.1016/j.ymssp.2019.106451)
- [9] Moharrami, M. J.; Martins, C. de A.; Shiri, H. (2021). Nonlinear integrated dynamic analysis of drill strings under stick-slip vibration, *Applied Ocean Research*, Vol. 108, Paper 102521, 13 pages, doi:[10.1016/j.apor.2020.102521](https://doi.org/10.1016/j.apor.2020.102521)
- [10] De Moraes, L. P. P.; Savi, M. A. (2019). Drill-string vibration analysis considering an axial-torsional-lateral nonsmooth model, *Journal of Sound and Vibration*, Vol. 438, 220-237, doi:[10.1016/j.jsv.2018.08.054](https://doi.org/10.1016/j.jsv.2018.08.054)
- [11] Richard, T.; Detournay, E. (2000). Stick-slip motion in a friction oscillator with normal and tangential mode coupling, *Comptes Rendus de l'Académie des Sciences – Series IIB – Mechanics*, Vol. 328, No. 9, 671-678, doi:[10.1016/S1620-7742\(00\)01240-X](https://doi.org/10.1016/S1620-7742(00)01240-X)

- [12] Richard, T.; Germay, C.; Detournay, E. (2007). A simplified model to explore the root cause of stick-slip vibrations in drilling systems with drag bits, *Journal of Sound and Vibration*, Vol. 305, 432-456, doi:[10.1016/j.jsv.2007.04.015](https://doi.org/10.1016/j.jsv.2007.04.015)
- [13] Sharma, A.; Al Dushaishi, M. F.; Nygaard, R. (2024). Evaluating PDC bit-rock interaction models to investigate torsional vibrations in geothermal drilling, *Geothermics*, Vol. 122, Paper 103060, 13 pages, doi:[10.1016/j.geothermics.2024.103060](https://doi.org/10.1016/j.geothermics.2024.103060)
- [14] Lerher, T.; Grum, Z.; Motaln, M.; Zadavec, M. (2024). Wear simulation of the conveyor belt transfer chute using the DEM, *International Journal of Simulation Modelling*, Vol. 23, No. 1, 77-88, doi:[10.2507/IJSIMM23-1-673](https://doi.org/10.2507/IJSIMM23-1-673)
- [15] Zhang, H.; Ni, H.-J.; Huang, B.; Liu, S.-B.; Wang, Y.; Liang, H.-J.; Guo, X. (2022). Research on discrete element modeling and numerical simulation of cutting rock behavior under impact load, *Energy Science & Engineering*, Vol. 10, No. 7, 2420-2436, doi:[10.1002/ese3.1146](https://doi.org/10.1002/ese3.1146)
- [16] Zhang, H.; Ni, H.-J.; Wang, Z.-Z.; Huang, B.; Liu, S.-B.; Xu, X.-Y.; Liu, C.-F. (2022). Discrete element modeling and simulation study on cutting rock behavior under spring-mass-damper system loading, *Journal of Petroleum Science and Engineering*, Vol. 209, Paper 109872, 14 pages, doi:[10.1016/j.petrol.2021.109872](https://doi.org/10.1016/j.petrol.2021.109872)
- [17] Huang, B.; Ni, H.-J.; Jin, Y.; Lu, Y.-H. (2024). The integrated drill string dynamic model based on the lumped mass method and discrete element method, *Mechanical Systems and Signal Processing*, Vol. 221, Paper 111723, 35 pages, doi:[10.1016/j.ymsp.2024.111723](https://doi.org/10.1016/j.ymsp.2024.111723)
- [18] Jaime, M. C.; Zhou, Y.-N.; Lin, J.-S.; Gamwo, I. K. (2015). Finite element modeling of rock cutting and its fragmentation process, *International Journal of Rock Mechanics and Mining Sciences*, Vol. 80, 137-146, doi:[10.1016/j.ijrmms.2015.09.004](https://doi.org/10.1016/j.ijrmms.2015.09.004)
- [19] Xiang, C.-Y.; Fang, P.; Li, H.-T.; Feng, H.; Tang, B.; Zhang, T.; Xiao, G.-L. (2023). Nonlinear dynamics of a drill string system with PDC bit in curved wells based on the finite element method, *Geoenergy Science and Engineering*, Vol. 230, Paper 212240, 18 pages, doi:[10.1016/j.geoen.2023.212240](https://doi.org/10.1016/j.geoen.2023.212240)
- [20] Liu, J.; Wang, J.-X.; Guo, X.-Q.; Dai, L.-M.; Zhang, C.; Zhu, H.-Y. (2022). Investigation on axial-lateral-torsion nonlinear coupling vibration model and stick-slip characteristics of drilling string in ultra-HPHT curved wells, *Applied Mathematical Modelling*, Vol. 107, 182-206, doi:[10.1016/j.apm.2022.02.033](https://doi.org/10.1016/j.apm.2022.02.033)
- [21] Zhang, H.; Di, Q.-F.; Li, N.; Wang, W.-C.; Chen, F. (2020). Measurement and simulation of nonlinear drillstring stick-slip and whirling vibrations, *International Journal of Non-Linear Mechanics*, Vol. 125, Paper 103528, 14 pages, doi:[10.1016/j.ijnonlinmec.2020.103528](https://doi.org/10.1016/j.ijnonlinmec.2020.103528)
- [22] Wang, B.-J.; Wang, Z.-Y.; Ren, F.-S. (2020). Dynamic model and quantitative analysis of stick-slip vibration in horizontal well, *Shock and Vibration*, Vol. 2020, Paper 8831111, 14 pages, doi:[10.1155/2020/8831111](https://doi.org/10.1155/2020/8831111)
- [23] Li, S.-Q.; Chen, Z.; Li, W.; Yan, T.; Bi, F.-Q.; Tong, Y.-S. (2023). An FE simulation of the fracture characteristics of blunt rock indenter under static and harmonic dynamic loadings using cohesive elements, *Rock Mechanics and Rock Engineering*, Vol. 56, No. 4, 2935-2947, doi:[10.1007/s00603-022-03214-x](https://doi.org/10.1007/s00603-022-03214-x)
- [24] Li, S.-Q.; Yan, L.-P.; Li, W.; Zhao, H.; Ling, X. (2019). Research on energy response characteristics of rock under harmonic vibro-impacting drilling, *Journal of Vibration Engineering & Technologies*, Vol. 7, No. 5, 487-496, doi:[10.1007/s42417-019-00146-9](https://doi.org/10.1007/s42417-019-00146-9)
- [25] Zhang, H.; Ni, H.-J.; Yang, H.-L.; Fu, L.; Wang, Y.; Liu, S.-B.; Huang, B.; Wang, Z.-X.; Chen, G. (2023). Numerical simulation and field test research on vibration reduction of PDC cutting of pebbled sandstone under composite impact load, *Processes*, Vol. 11, No. 3, Paper 671, 19 pages, doi:[10.3390/pr11030671](https://doi.org/10.3390/pr11030671)
- [26] Xi, Y.; Wang, H.-Y.; Zha, C.-Q.; Li, J.; Liu, G.-H.; Guo, B.-Y. (2023). Numerical simulation of rock-breaking and influence laws of dynamic load parameters during axial-torsional coupled impact drilling with a single PDC cutter, *Petroleum Science*, Vol. 20, No. 3, 1806-1827, doi:[10.1016/j.petsci.2023.01.009](https://doi.org/10.1016/j.petsci.2023.01.009)
- [27] Kang, H.-P.; Jiang, P.-F.; Huang, B.-X.; Guan, X.-M.; Wang, Z.-G.; Wu, Y.-Z.; Gao, F.-Q.; Yang, J.-W.; Cheng, L.-X.; Zheng, Y.-F.; Li, J.-Z. (2020). Roadway strata control technology by means of bolting-modification-destressing in synergy in 1000 m deep coal mines, *Journal of China Coal Society*, Vol. 45, No. 3, 845-864, doi:[10.13225/j.cnki.jccs.SJ20.0204](https://doi.org/10.13225/j.cnki.jccs.SJ20.0204)